

# Design and Analysis of Graded Honeycomb Shock Absorber for Increasing the Safety of Passengers in Armored Vehicles Exposed to Mine Explosion

S.A. Galehdari<sup>1,\*</sup>, H. Khodarahmi<sup>2</sup>, A. Atrian<sup>1</sup>

<sup>1</sup>Modern Manufacturing Technologies Research Center, Najafabad Branch, Islamic Azad University, Najafabad, Iran

<sup>2</sup>Department of Mechanical Engineering, I H University, Tehran, Iran

Received 10 March 2017; accepted 8 May 2017

## ABSTRACT

Protecting armored vehicles from mine explosion can lead to the survival of thousands of people exposed to this risk. Very purpose, shock absorbers such as honeycomb structures can be applied for crashworthiness improvement. In this study, graded honeycomb structure is primarily introduced as a shock absorber, followed by the introduction of its absorbed energy and the force and acceleration applied to the occupant which is numerically simulated and measured in Abaqus software. In order to validate the numerical simulation results, a low-velocity experimental test has been conducted on a prototype, and the obtained results indicate well agreement with empirical results. In the meanwhile of mine explosion under a armored vehicle, it has been considered that the vehicle will be thrown upwards with a velocity of 10 m/s and will hit to the ground thereafter. For this case, a shock absorber has been designed, optimized and analyzed. According to the obtained results, the designed shock absorber meets all of the standard requirements. The applied simulation and design method can be further extended for miscellaneous shock absorbers.

© 2017 IAU, Arak Branch. All rights reserved.

**Keywords :** Graded honeycomb structure (GHS); Shock absorber; Armored vehicle; Mine explosion; Crashworthiness.

## 1 INTRODUCTION

**N**UMEROUS studies have been performed regarding the human body response to the effects of mine explosion under a vehicle and under its tires. Moreover, a plentitude of papers in military and civilian studies have been published in this specific field. To exemplify the case, NATO has evaluated the results of engineering field studies. The last step within the process of a mine explosion is the damage to the vehicle's occupants, while the aim of setting up mines in the route of a vehicle is the same issue. Hence, a detailed understanding of the influence of explosion wave on the human body should be achieved for the purpose of designing safer vehicles with respect to the human's tolerance threshold.

Regarding numerical analyses and conducted crash tests, legs as the primary shock recipient, hip which is being supported by the seat, spinal cord, neck, and skull are respectively the major parts undergoing severe injuries. Given the duration of force application, the highest injuries occur to the legs. Approximately 3 to 5 milliseconds after the explosion, the highest load –equal to 6KN- will be applied to the calves. Afterwards, 15 to 18 milliseconds after the explosion, a 4KN and a 1KN force will be applied to the spinal cord and the neck area, respectively [1]. In order to

\*Corresponding author. Tel.: +98 9399238836; Fax: +98 31 42292537.  
E-mail address: ali.galehdari@gmail.com (A.Galehdari).

evaluate the occurred injury to the body caused by the mine explosion, injury criteria, supporting surfaces of the body exposed to the acceleration, and the effect of the applied wave on them will be utilized.

A complete understanding of the effects of an explosion under a vehicle on its occupant derives from an attentive analysis of the explosion phenomenon. Nonetheless, it should be noted that relevant information are of high confidentiality; hence, published results do not consider complete details. Consequently, most of the studies have had the tendency of applying numerical methods. In these studies, a dummy is normally used with various types of sensors attached to different parts of them. To exemplify the case, a strain gauge attached to the dummy's calf can measure the strain, thus the applied stress and force to the leg, as well as its following movements after the explosion. This procedure can be extended for measurements of other parts of the body. The obtained values can be used as inputs for the simulation of applied forces to the human body. The magnitude of the applied forces to the occupant depend on the distance of the occupant and the explosion location, the structure of the vehicle, internal composition of the vehicle such as seats and their attachments therein, and the composition of plates under the feet of the occupant. If the seat or the location of the feet lies on a plate that deform due to the explosion, a great force will be applied to the feet, ankles, calves, and the knees. This force would result in an accelerating upward movement of the leg and hitting other internal parts of the vehicle. Pelvic floor is another organ which might experience severe loads. Considering the seat mounted and assembled onto the lower plate of the vehicle, the load caused by the explosion will reach the pelvic floor in 10 milliseconds. The magnitude of this load directly depends upon the suspension system of the vehicle. However, having the seat attached to the car on the ceiling would make this load to reach the pelvic floor by 15 to 30 milliseconds and a relatively lower magnitude [2]. Chen and Pugno[3] have studied in-plane elastic characteristics of Nano-honeycomb through analytical approach. In this paper, the influence of two geometrical parameters on the elastic characteristics of the structure has been studied. These two parameters are the ratio of stiffness to density, and the ratio of strength to the density of the structure. Given the represented theory, there is the feasibility of producing Nano-honeycomb structure. Additionally, Nakamoto et al.[4] have investigated the behavior of honeycomb structure filled with a solid material under in-plane impact loading. In this research, using finite element method, the effect of filler's characteristics on deformation, average stress, locking strain, and the absorbed energy of the structure have been studied. Increasing the volume of the filler material, the average stress and the locking strain have increased. The amount of absorbed energy as a function of the volume of the filler material has been represented within an analytical equation. In order to study the possibility of using soft Aluminum honeycombs, Tanaka et al.[5] studied this structure under in-plane impact loading. In this study, the functionality of this structure as a shock absorber in cars for rescuing humans involved in accidents. Moreover, conducting an empirical test, the characteristics of this type of deformation has been analyzed in the structure by the means of high velocity cameras. Given the ratio of strength to mass and the high specific energy of these structures, they have been increasingly used in aerospace industries. Veltin [6] studied the behavior of regular honeycomb structure under in-plane impact loading through simulation in Abaqus software. In this study, keeping constant the angle, the effect of cell's geometry on energy absorption has been investigated. This structure has also been applied as the shock absorber under helicopter seats. Sandwich structures which are considered as shock absorbers usually contain honeycombs in their core parts. In order to increase the energy absorption capacity, honeycomb structure with graded mechanical characteristics can be applied. Stromsoe [7] has studied the application of honeycomb in sandwich structures using numerical simulations in Abaqus software and applying graded structure for achieving highest levels of energy absorption. In this research, an in-plane loading has been applied on the sandwich structure.

In order to study the effect of element type within a honeycomb structure on the numerical results, Asadi et al. [8] have analyzed the application of honeycomb structure in a car bumper, in which the bumper went through crashes with four different velocities. The numerical simulation of this study has been conducted in LS Dyna software. Meshing the structure has been performed by two different types of continuous and shell elements. Regarding the geometry of the honeycomb structure, the results of shell element has had higher concordance with empirical results.

Mona et al. [9] analyzed the behavior of sandwich composite structure with a honeycomb core under impact loading, using experimental tests and numerical simulations in LS Dyna software. In the numerical simulation, for the meshing of plates and honeycomb, continuous and shell elements have been applied, respectively. The comparison of Force-Deformation diagrams and the deformed shape of the structure has revealed an appropriate concordance between numerical and empirical results. In order to study the behavior of honeycomb structure, its force-deformation diagram, and the deformation mode of its structure under quasi-static loading, Redzay et al. [10] conducted an experimental study on an aluminum honeycomb structure. A quasi-static loading on three principle directions was applied to the structure. Within the force-deformation diagram of the structure, three sections of elastic, flat, and locking are obvious. Chao et al.[11] have studied the compressive behavior and energy absorption

characteristics of high porosity closed-cell aluminum foam specimens subjected to low velocity impact loading. The dynamic deformation behavior of the specimen is observed by high speed camera and the velocity attenuation of the drop hammer is recorded. The results demonstrate that the aluminum foam has excellent energy absorption capabilities under low velocity impact loadings, with its dynamic compression behavior similar to that obtained under quasi-static loading conditions.

Shariyat et al.[12] have investigated on influences of the in-plane biaxial compression, tension, or tension-compression preloads on various responses of the low-velocity impact. In this paper different contact laws are considered for the loading and unloading phases. Results show that the compressive and tensile in-plane preloads reduce and increase the contact force, respectively. Rezaie Pour Almasi et al.[13] have used optimization methods to change the modified stress-strain curved in a way that the shape resulting from simulation coincides with the sample resulting from the test. The optimization results have been verified by analytical ones. Galehdari et al. [14] have presented an objective function for GHS optimization problem. In this research the specific absorbed energy of the structure has been optimized. The optimization problem has been performed by two algorithms.

Inspired from the sponge structure of banana peel, Muhammad Ali [15] has introduced a graded honeycomb structure as demonstrated in Fig. 1. In this structure, the thickness of rows has increased from bottom to the top.

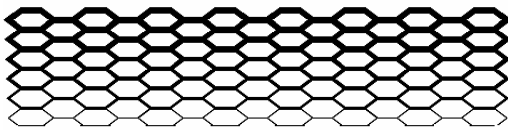


Fig.1  
The modified peel structure [15].

Galedari et al. [16] studied the energy absorption of this structure by considering a material model with power hardening. In this study, based upon the mentioned material model, a relation for the specific absorbed energy of the structure (Eq.1) has been derived. The analytical results from this equation hold a well agreement with numerical results.

$$e = \frac{U}{m} = \frac{AL \sum_{i=1}^n \sigma_{p_i} \frac{\varepsilon_{d_i}}{n}}{m} \quad (1)$$

where  $\sigma_{p_i}$  is the plateau stress of each row for the material model with power hardening,  $\varepsilon_{d_i}$  is the corresponding locking strain for each row,  $A$  is the cross section of the structure perpendicular to the longitudinal direction and  $L$  is the structure height in longitudinal direction (direction of collision). They also studied the effect of in-plane loading and structural grading on GHS respond. In this study, structural grading and the in-plane loading reduce the amount of transmitted force and it's time duration. For the graded structure the force is transferred smoother and lower rather than the same thickness one [17]. In another research, they have performed quasi-static test on GHS test specimen. The experimental results have good agreement with analytical results. Analytical results has been reported for plateau stress[18].

Anti tank (AT) mines and improvised explosive devices (IED) pose a serious threat to the occupants of infantry vehicles. The use of an energy absorbing seat in conjunction with vehicle armor plating greatly improves occupant survivability during such an explosion. Tabiei et al.[19] have investigated the dynamic axial crushing of aluminum tubes constitutes the principal energy absorption mechanism to reduce the blast pulse transmitted to the occupant. The injury mechanisms of both vehicle-occupant has been simulated with FEM. Data such as hip and knee moment, femoral force, and foot acceleration is collected from the numerical dummy which simulates the occupant's response. This data is then compared to injury threshold values from various references to assess survivability.

The analysis of contemporary military conflicts shows, that the most dangerous threat for soldiers are Improvised Explosive Devices (IEDs). To design and develop better protection system it is necessary to identify and measure the effects of blast wave impact on crew of military vehicle. Sławiński et al.[20] have numerically simulated a armoured vehicle subjected to mine threat of 8 and 10 kg of TNT. The effects of mine explosion on human body are studied. The analysis is simulated using LS-DYNA software. Only vehicle's hull is considered with suspension and turret is modelled using mass. Accelerations and forces in tibia, neck and spine were calculated. HIC-36 criterion was also evaluated different types of possible seat configuration are investigated. Results show convergence between explosive size and injury risk.

In the case of designing shock absorbers for the protection of human body, reaction force must be considered as well as the amount of absorbed energy. In this research, the design of shock absorbers under armored vehicle seats has been investigated. During mine explosion crash, the vehicle will be thrown upwards with a velocity of 10 m/s and will hit to the ground thereafter. So the impact energy would be applied to the seat and to the occupant. Hence, the amount of absorbed kinetic energy and the transferred force must be regarded during the design of shock absorbers. In-plane loading, in contrast with out-of-plane loading, applies a lower force to the protected part, considering specific energy absorption. On the other hand, grading the structure ensures that the application of reaction force to the protected part would happen with a lower rate and within a longer duration. Given the above-mentioned features for graded honeycomb structure, a shock absorber for armored vehicle crash has been designed and analyzed based upon vehicle standards.

## 2 EXPERIMENTAL TEST

In order to validate the numerical simulation method in Abaqus software, an experimental test has been conducted as the falling a weight with low velocity on a graded honeycomb structure. The experimental model is a 6061-O aluminum GHS. This structure has 6 rows with different thicknesses. The rows are glued to each other by Adhesive-Film. The thickness of 1st to sixth rows is 1.6, 1.27, 1.016, 0.8125, 0.635 and 0.508 mm, respectively. For this model  $c=15$ ,  $l=12$ ,  $b=28.5\text{mm}$  and the height and width are 130 and 130 mm, respectively. This structure is demonstrated in Fig. 2.

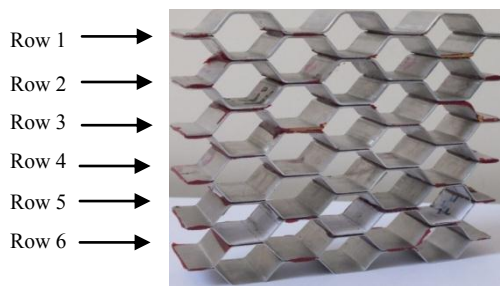


**Fig.2**  
Test sample of 6-row graded honeycomb structure.

To determinate the characteristics of this alloy for a more precise analysis, the materials of all of six thicknesses have been analyzed under a tension test using Santam machine. The mechanical characteristics of each row have been listed in Table 1. It is noteworthy that the density and Poisson ratio of this aluminum are  $2700\text{ kg/m}^3$  and 0.33, respectively. The obtained mechanical properties are used to define the material properties in finite element simulation. Low velocity impact test has been performed by drop hammer test device. In this test, 99 Joule kinetic energy was applied to the GHS. A system of 9776.6 gr has dropped from a 1.2 m height. The acceleration of the block has been recorded during the impact to the structure and energy absorption by an accelerometer based on these results, force-displacement diagram was sketched.

**Table 1**  
Mechanical properties of different thickness of AL6061-O plate.

Thickness(mm)	$E(\text{GPa})$	$n$	$K(\text{MPa})$	$e_f\%$	$S_{ut}(\text{MPa})$	$S_y(\text{MPa})$
1.6	68.28	0.213	202.77	23.76	131.39	51.59
1.27	66.98	0.245	242.66	25.142	141	51.92
1.016	62.5	0.291	220.8	25.168	131	50.7
0.8125	63.51	0.229	205.6	30.72	141	50
0.635	64.3	0.247	228	27.06	134	48.15
0.508	66.81	0.303	217.27	31.092	124	53

Regarding the material and geometrical characteristics of the structure, the mass and the velocity of the weight, loading and boundary conditions, the experimental test on the sample has been simulated in Abaqus Software. The FE model made of aluminum 6061-O of graded honeycomb structure is demonstrated in Fig. 3. The dropped mass and the structure base are modeled by plate A and B, respectively. Hourglass controlled, 8 nodes, reduced integration linear brick elements (C3D8R) are used to mesh the structure and rigid bilinear quadrilateral elements (R3D4) are

used to mesh plate *A* and plate *B*, respectively. The structure wall is nearly thick here and the C3D8R element is used. The boundary conditions are defined by constraining the discrete rigid plate, *A*, to move only in the *Y* plane and by fixing all the rotational and translational degrees of freedom of the discrete rigid plate, *B*. Using the measured material properties the plastic behavior of AL-6061O is defined using power hardening model for each row individually. The finite element problem is solved by dynamic/explicit solver.

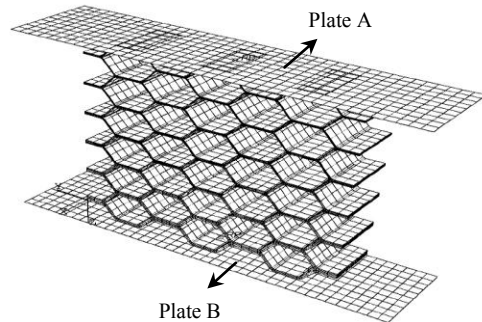


**Fig.3**  
FE model of GHS.

### 3 DESIGN OF SHOCK ABSORBER

According to the mentioned capabilities of graded honeycomb shock absorber, a type of this absorber has been designed and analyzed in order for being used in armored vehicle. Applying this shock absorber under the seat results in the absorption of the explosion energy and prevents injuries to the occupant by a more gradual applying of the load. Regarding the fact that this 15ton armored vehicle does not benefit from a suspension system, one has been primarily designed and analyzed for it. Following the study of the absorbed energy by the suspension system, the energy absorbed by the shock absorber has been under scrutiny. In order to verify the safety of a potential occupant, the applied load, HIC parameter, and the acceleration changes have been measured and compared to corresponding standard values.

#### 3.1 Problem definition

An armored vehicle may go through a mine explosion, during which the vehicle will be thrown upward. This sudden movement besides the subsequent hitting of the vehicle to the ground would cause significant injuries to the occupant; thus, the occupant must be protected by the means of providing specific safety features to the vehicle. Given the available information, the maximum explosive material for a 15ton armored vehicle is 8 kg of T.N.T. Following the conducted numerical simulations in Auto Dyne software, the explosion of 8 kilograms of T.N.T would cause the armored vehicle to be thrown upward with a velocity of 10 m/s [21]. In case of a non-vertical movement occurring, the vertical velocity will be lower than 10 m/s. In order to make a conservative design, it has been assumed that the rise and the chute of the vehicle would happen in vertical direction. Following the hitting of the vehicle to the ground with a velocity of 10 m/s, based upon Eq. (2), the kinetic energy of  $7.5e5 J$  will be applied to the vehicle.

$$K.E = \frac{1}{2}mv^2 = \frac{1}{2}15000 \times 10^2 = 7.5 \times 10^5 j \quad (2)$$

A quarter of the vehicle has been considered within the modeling for the sake of simplicity. Therefore, the energy absorption of 187500 J has been analyzed for the quarter model. In order to study the energy absorption, the characteristics of the suspension system of the vehicle should be available. Since no suspension system has been previously designed for the vehicle, the required characteristics could be considered in addition to the characteristics of the tire. The remaining kinetic energy after the suspension system performance should be absorbed by the shock absorber beneath the seat, and the desirable graded honeycomb shock absorber has been accordingly designed,

optimized and analyzed. Of note is that the least energy should be transferred to the occupant during the energy absorption; thus, injury parameters should be calculated and compared to standard criteria values.

### 3.2 Design and simulation of armored vehicle suspension system

#### 3.2.1 Vehicle suspension system design

In order to design a suspension system, the mass/spring model of the vehicle should be primarily studied. For heavy vehicles, leaf springs and air dampers are highly applicable. In this modeling, leaf spring and air damper have been respectively equalized with helical spring and hydraulic damper. Accordingly, the mass/spring model of the car has been considered as demonstrated in Fig. 4.

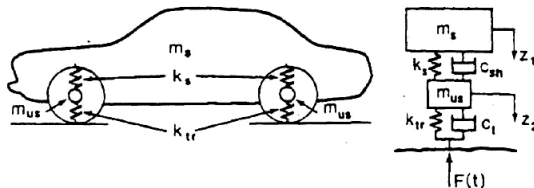
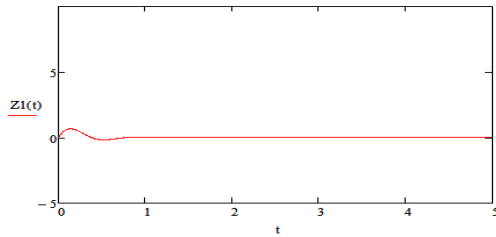


Fig.4  
Suspension system of a car.

For determining the unsprung mass, regarding the study performed by Huang [22], the unsprung mass is approximately 17.7% of the vehicle's total mass. The spring and unsprung masses of vehicle are  $m_s = 3086.2$  and  $m_{us} = 663.8 \text{ kg}$ . Using the available catalogs for 15ton heavy truck and corresponding tire catalogs from Michelin Company, Michelin 368/80/R22.5 radial tire has been selected [23]. Given the type of the selected tire, as well as its available characteristics, the damping coefficient and stiffness of the tire can be obtained as  $k_{tr} = 8.74 \times 10^5 \text{ N/m}$  and  $c_{tr} = 6600 \text{ N.s/m}$  [24]. The distance of spring mass to the unsprung one, and the unsprung mass down to the ground has been determined regarding the characteristics of the tire. The width of the selected tire is 368 mm, and its height in inflated condition is  $0.8 \times 368 = 294.4 \text{ mm}$ . As well, the ring diameter equals 22.5 inches (571.5mm). It is noteworthy that the distance between the unsprung mass to the ground equals the height of the tire [25]. On the other hand, it should be mentioned that the distance between the spring mass and the ground is approximately equal to the summation of ring radius and the unsprung distance. These two distances are  $h_s = 294.4$  and  $h_{us} = 865.9 \text{ mm}$ . After the determination of several input parameters of the problem, it is required that the spring stiffness and the damping coefficient of the vehicle's damper be calculated. For this very purpose, the displacement of the vehicle ( $Z_1$ ) in free vibrations should reach one tenth of its amplitude within at least 5 seconds. This would imply that the designed suspension system meets the requirements and can control the vibrations and vehicle displacements within an appropriate time period. Hence, the one-DOF vibrations of the suspension system of the vehicle have been analyzed and its time response,  $Z_1(t)$ , has been derived. The final equation of the vibration system response is represented in Eq.(3).

$$Z_1(t) = e^{-\zeta \omega_n t} \left( \frac{10}{\omega_n \sqrt{1-\zeta^2}} \sin \omega_n t \sqrt{1-\zeta^2} \right) \quad (3)$$

In Eq.(3), two parameters of  $K_s$  and  $C_{sh}$  are the variables and have been determined through try and error, in a way that the displacement of the vehicle ( $Z_1$ ) reach one tenth of its initial amplitude within at least 5 seconds. Through programming in Mathcad software,  $c_{sh} = 27 \times 10^3 \text{ N.sec/m}$  and  $k_s = 3 \times 10^5 \text{ N/m}$  have been calculated. The vibration system response as a function of time has been demonstrated in Fig. 5, obtained in Mathcad software.



**Fig.5**  
Diagram of vehicle displacement as a function of time for free vibrations.

Given Fig.5, the vehicle displacement has been thoroughly damped within a fraction of a second, and its amplitude has consequently reached zero. Therefore, the designed suspension system meets the requirements and is acceptably practical and appropriate.

3.2.2 Simulation of energy absorption for vehicle’s suspension system

In order to determine the percentage of absorbed energy by the suspension system after the crash of vehicle to the ground, this system has been simulated in Abaqus software, in which the 2 DOF suspension system has been modeled as represented in Fig. 4. The applied damping coefficient and the hardness of the tire and the suspension system have been as for previous section. For simulating the designed suspension system in Abaqus software, spring and non-spring masses have been considered as two rigid parts with concentrated mass, and the required springs and dampers have been inserted between them. It should be mentioned that the modeled spring and damper are just a connector. Furthermore, these connectors have not been meshed in the software, and have undergone complete deformations after the load application. In order words, the initial static length has not been considered for the spring. Therefore, the initial static length should be subtracted from the initial length for determining the distance between two masses (spring length).

For the length of the spring corresponding to the tire, and for the length of spring in the suspension system, the tire thickness and the static length have been respectively subtracted from this length. Hence, the initial length of the springs has been considered as  $h'_s = 762\text{mm}$  and  $h'_{us} = 212\text{mm}$ . Modeling of vehicle suspension system and the tire in Abaqus software are represented in Fig. 6.

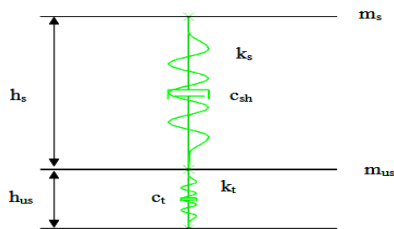


**Fig.6**  
Modeling of vehicle suspension system and tire in Abaqus software.

The demonstrated system in Fig. 6 hits the ground with a velocity of 10 m/s. Following the numerical simulation in this software, it has been observed that after hitting the ground and a couple of oscillations in the direction of vehicle’s displacement, the suspension system has absorbed 185447J out of 187500J total kinetic energy. The diagram of changes in kinetic energy of the entire system and the suspension system as a function of time is demonstrated in Fig. 7.

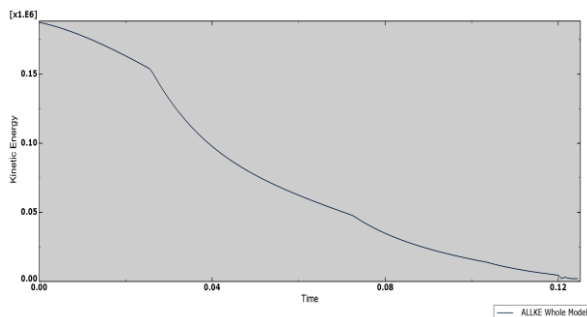


**Fig.7**  
Kinetic energy of the quarter model of the vehicle as a function of time after hitting the ground with the velocity of 10 m/s.

Given Fig. 7, the suspension system has absorbed a plentitude of the applied kinetic energy to the vehicle. The remaining kinetic energy which is 2053J will cause severe injuries in case of being applied to the occupant directly. In the following section, a graded honeycomb structure will be designed in a way that the least possible kinetic energy be applied to the occupant, and causing the lowest potential injuries, consequently.

### 3.3 Design and simulation of graded honeycomb shock absorber for occupant seat

In designing shock absorbers for cases having the purpose of human body protection, the reaction force should be regarded as well as the energy absorption. At the moment when vehicle hits the ground, the impact load will be applied to the suspension system, the seat, and the occupant, respectively. Thus, the design of shock absorber should include details considering this transferred load. By grading the structure, the reaction force would be transferred to the occupant with a lower rate and within a longer time. Given the aforementioned for the graded honeycomb structure, a shock absorber based upon the available standards for the crashing vehicle and its occupant has been designed and analyzed.

During a crash, drastic injuries could occur to a occupant, which is the reason for the codification of standards determining the allowed injury to the occupant. Given the available resources, a number of these limitations have been explicated below.

- The maximum applied acceleration in the direction of the impact shall not exceed 7.88g (DRIZ<7.88g). Considering an average mass of 77 Kg for the occupant, the applied force to the hip must not exceed 5952N ( $F_{z \max} < 7.88 \times 9.81 \times 77 = 5952N$ )
- Acceleration change in a period of 7 milliseconds shall not exceed 23g.
- During the crash, the head of the occupant must not hit any part within the vehicle. Otherwise, the head injury criteria (HIC) shall be lower than 1000. The equation for this criterion is represented in Eq.(4). Of note is the fact that in this equation,  $t_2 - t_1 \leq 0.05$  second [26-28].

$$HIC = (t_2 - t_1) \left[ \frac{1}{t_2 - t_1} \int_{t_1}^{t_2} a(t) dt \right]^{2.5} \quad (4)$$

#### 3.3.1 Design of seat shock absorber

For a conservative design, it has been assumed that the entire applied kinetic energy is absorbed by the shock absorber, and the energy absorption by the legs of the seat is neglected. The mass of the occupant is considered 77 Kg and the impact velocity is 10 m/s. Therefore, the applied energy to the shock absorber can be calculated based upon Eq.(1).

##### 3.3.1.1 Optimized design

In designing shock absorbers, it is required to select the structure's geometry and material in a way that the specific energy of the structure always remains maximum. Accordingly, the structure optimization has been performed regarding the obtained analytical equations. During the design process, the shock absorber thickness is selected similar to that of the empirical test sample. Therefore, the thicknesses of 1.6, 1.27, 1.016, 0.8125, 0.635, and 0.508 mm have been used for each row of the structure.

It is required to maximize the specific energy by changing geometrical parameters. The structure undergoes the impact of a plate with the mass of 77 Kg and initial velocity of 10 m/s. the purpose of optimization in this step is minimizing the ratio of mass to the absorbed energy by the structure. For designing the shock absorber, optimization has been performed using Genetic and Sequential Quadratic Programming (SQP) algorithms in MATLAB. For both of these algorithms, the objective function is the ratio of the mass to the absorbed energy of the structure as shown in Eq.(5).

$$e = \frac{U}{m} = \frac{2bl \cos \phi (15c + 16l \sin \phi) \sum_{i=1}^6 K_i \sigma_{pi} \epsilon_{di}}{\rho b (32l + 23c) \sum_{i=1}^6 d_i} \quad (5)$$



In the equation above,  $K_i$  is the number of rows in each of the six determined thicknesses. In order to apply the influence of bending moment on the structure's deformation, the condition of should be met. Regarding the articles of the standard, the reaction force to the pelvis of the occupant must be less than 6674N. Also the structure should be capable of absorbing a minimum of 2391.15J of the kinetic energy. For both algorithms the optimization problem is

$$\text{defined as: } \min \frac{[m(X_i)]}{U(X_i)}$$

st.

$$\frac{d}{l} < 0.25$$

$$\sigma_p A < 5952N$$

$$U = 2053j$$

$$2 * l * \cos(\phi) * \left( \sum_{j=1}^6 K_j \right) = 0.5m, j = 1, 2, \dots, 6$$

$$lb \leq X_i \leq ub, i = 1, 2, \dots, 15$$

(6)

Design variables are provided in Table 2. The upper and lower boundaries of the variables are equal to vectors  $ub$  and  $lb$ , respectively.

$$lb = [0.015, 0.012, 0.628, 0.00023, 0.000235, 0.00024, 0.000245, 0.00025, 0.000255, 1, 2, 3, 4, 4, 16]$$

$$ub = [0.025, 0.02, 0.7, 0.000235, 0.00024, 0.000245, 0.0002, 5, 0.000255, 0.00026, 2, 5, 5, 7, 7, 20]$$

The optimization is conducted by two genetic and SQP algorithms and their results are compared to each other. In genetic algorithm, a generation of 50 and two stopping criteria are applied as a maximum number of 100 generations. The number of continuous generations without a change in optimum point reaches 9. A constraint and function tolerance of  $10^{-9}$  is applied. In SQP method, the constraint and function tolerance equal to  $10^{-6}$  and the start point equal to lower limit ( $lb$ ) is considered.

**Table 2**

Design variables in optimizing the helicopter seat shock absorber.

Geometric parameter	Design variable		Geometric parameter	Design variable	
$x(1)$	$c$	Cell horizontal wall length	$x(10)$	$K_1$	Number of rows with $d_i$ thickness
$x(2)$	$l$	Cell inclined wall length	$x(11)$	$K_2$	
$x(3)$	$\varphi$	Cell wall angle	$x(12)$	$K_3$	
$x(4)$	$d_1$		$x(13)$	$K_4$	
$x(5)$	$d_2$		$x(14)$	$K_5$	
$x(6)$	$d_3$	Cell wall thickness	$x(15)$	$K_6$	
$x(7)$	$d_4$				
$x(8)$	$d_5$				
$x(9)$	$d_6$				

### 3.3.1.2 Numerical simulation

In order to evaluate the optimization results, the designed model has been simulated in Abaqus software. For the purpose of meeting the requirements of the standard, the diagrams of reaction force, acceleration, and kinetic energy should be derived as a function of time. According to the results of the optimization, the geometry of each row is demonstrated in Fig. 8.

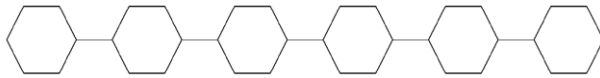


**Fig.8**  
Geometry of one row of armored vehicle seat shock absorber.

Regarding the conducted design, the entire structure consists of 30 rows. The material of all of the rows is AL6061-0. The material properties of each row with specific thickness are considered as of the properties mentioned in Table 1. A scheme of the designed shock absorber is represented in Fig. 9.

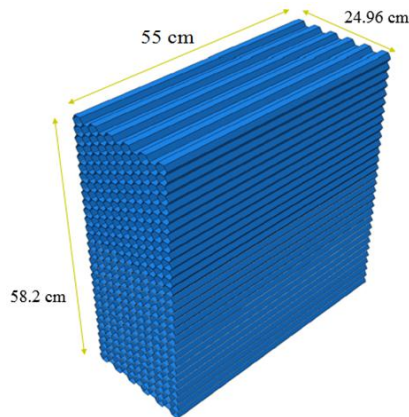


**Fig.9**  
Geometrical model of the armored vehicle seat shock absorber.

For meshing the structure, the four-node shell element of S4R, and for rigid plates *A* and *B*, the bilinear and four-node element of R3D4 has been used. Applying the impact loading to the structure has been realized by the upper plate *A* with a mass of 77kg and a velocity of 10 m/s; while the interaction of the shock absorber with the occupant has been simulated by the lower plate *B*. The interaction of plate *A* and the structure is a kinematic surface-to-surface contact, and the interaction of plate *B* to the structure, a frictionless penalty contact has been defined. Defining boundary conditions on plate *A*, motion is only allowed in *Y*-direction (impact direction) while all degrees of freedom are fixed for plate *B*.

#### 4 RESULTS AND DISCUSSION

In this simulation, the final reaction force and deformation of the structure obtained from numerical solution is compared to the experimental results in Table 3. Fig.10 illustrates the obtained deformed shapes of numerical simulation and experimental tests at 2.4 ms.

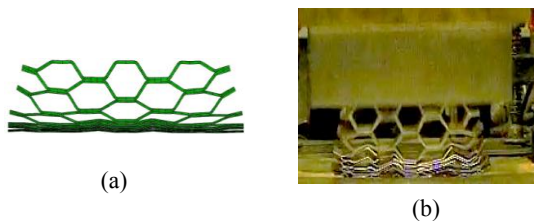


**Fig.10**  
Deformed shape of GHS under low-velocity impact load; (a) Numerical simulation, (b) Experimental test.

**Table 3**  
Final reaction force and deformation magnitude for experimental test and numerical.

Variable	Numerical	Experimental	Error%
Final reaction force (N)	2248	2128	5.3
Final Deformation (mm)	91.24	94.5	3.4

According to Fig. 10, and Table 3. the numerical, experimental and analytical results retain an appropriate congruence. Moreover, the deformed shape of test sample obtained from experimental test has an acceptable similarity with the numerical deformed shape. However, the obtained congruence of analytical and numerical results with experimental ones would be a robust support for the represented analytical and numerical simulation method. The optimization problem using Genetic algorithm with an initial population of 50 has been defined with the stopping criteria of the maximum produced generations reaching 100 and the number of continuous generations reaching 9 without the change of optimum point. The optimization has stopped after the production of 56 generations while meeting the second stop criterion. The ratio of the mass to the absorbed energy of the structure has been calculated as  $0.0031 \text{ kg/j}$ . the optimization problem using SQP algorithm with a function and constraint tolerance of  $10^{-6}$  and the starting point equal to lower boundary ( $lb$ ) has stopped after 187 iterations with the function and constraint tolerance stopping criterion. The ratio of the mass to the absorbed energy of the structure has been calculated as  $0.0036 \text{ kg/j}$ . Table 4. represents the obtained design parameters from two optimization algorithms. Comparing the obtained results from Genetic and SQP algorithms, since the ratio of the mass to the absorbed energy of the structure has been higher in Genetic algorithm compared to that of SQP algorithm, the results of Genetic algorithm have been considered as optimum ones.

A scheme of the deformed structure after complete absorption of applied kinetic energy is shown in Fig. 11. The acceleration diagram, reaction force applied to the occupant and the kinetic energy as a function of time are also demonstrated in Fig. 12.

**Table 4**  
Obtained design parameters from Genetic and SQP algorithms.

Design variable	Optimized value by GA	Optimized value by SQP
$c$	15 mm	18.04 mm
1	12 mm	12.17 mm
$\varphi$	30°	30.8°
$d1$	0.25 mm	0.2408 mm
$d2$	0.255 mm	0.2549 mm
$d3$	0.26 mm	0.255 mm
$d4$	0.265 mm	0.2646 mm
$d5$	0.27 mm	0.2695 mm
$d6$	0.277 mm	0.2751 mm
$K1$	1	2.569
$K2$	2	3.628
$K3$	3	4.6
$K4$	4	5.592
$K5$	7	8.59
$K6$	13	14.39

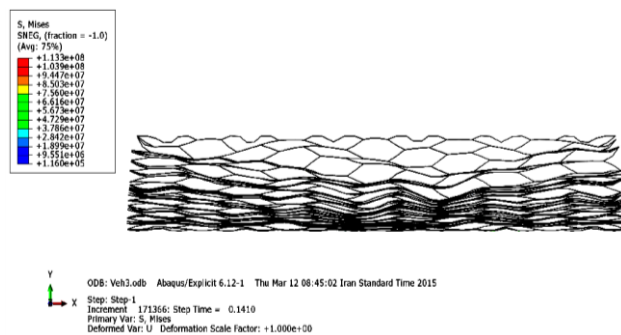


**Fig.11**  
Scheme of deformed structure after the complete absorption of kinetic energy.

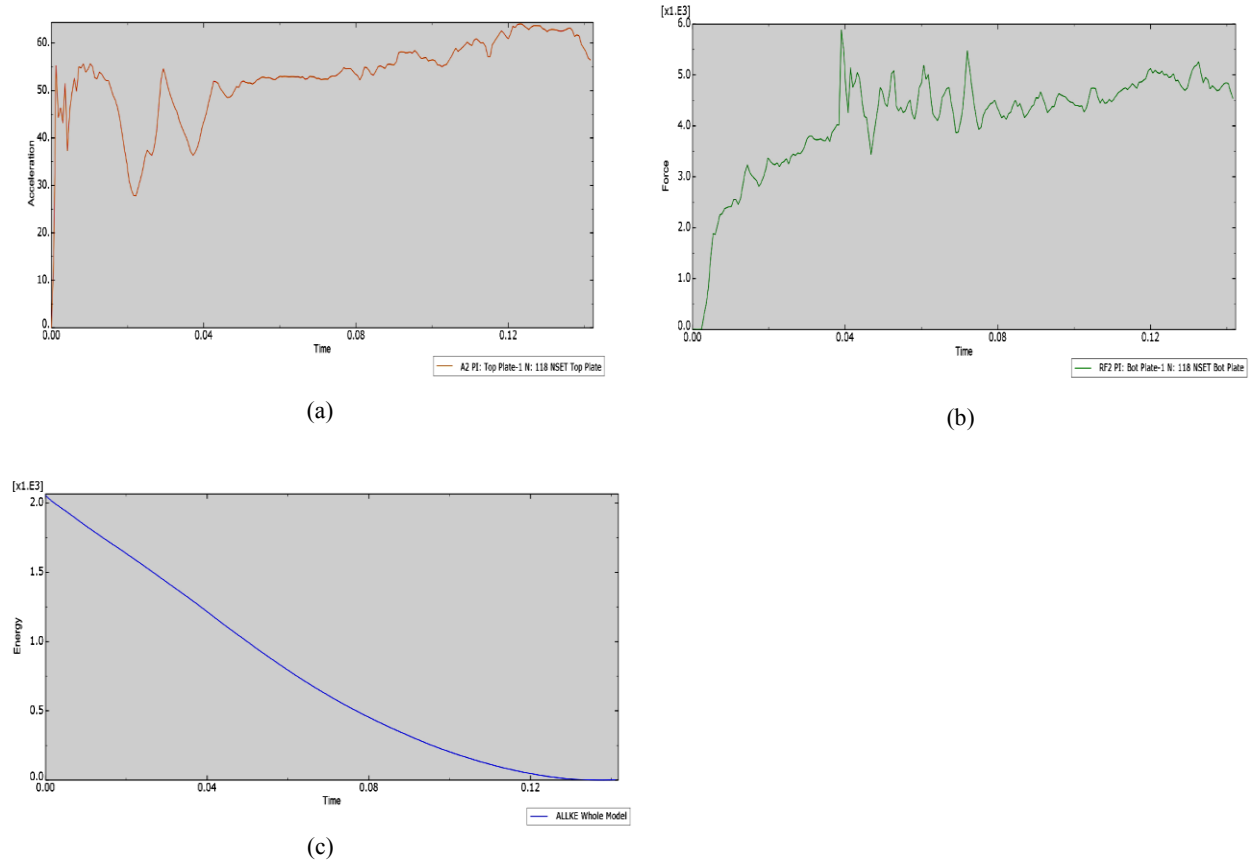
**Fig.12**

Diagram a) Applied acceleration to the occupant, b) Applied reaction force to the occupant, c) Kinetic energy as a function of time.

Given the above-mentioned article (a), the applied force to occupant's pelvis should not exceed  $5952N$ . According to Fig. 12(b), the maximum reaction force is  $5882N$  which is lower than the allowance limit. Therefore, this section of the standard is also satisfied through the designed shock absorber.

According to the article (b) of mentioned standard, the acceleration change applied to the occupant in duration of 0.007 second should be less than  $23g$ . Based on Fig. 12(a), the acceleration changes in this time period is  $5.6g$  which is far less than  $23g$ . Hence, this part of the standard has been met by the designed absorber.

Regarding Fig. 12(c), the entire  $2391.15J$  amount of kinetic energy has been absorbed; thus, the design is appropriate in terms of the absorbed energy as well.

Considering article (c) of standard, HIC parameter is not permitted to exceed 1000. Based upon Fig.12(a) and numerical integration in MATLAB software, the value of this parameter for the designed absorber is 673.24 which is lower than the determined limit. This section of the standard is accordingly satisfied by the designed absorber.

Consequently, the designed shock absorber meets all of the articles of vehicle crash standards, and could be applied under a armored vehicle seat as the shock absorber in case of crash conditions.

## 5 CONCLUSIONS

The appropriate concordance between the empirical results and those of numerical simulation for energy absorption of a graded honeycomb structure indicates the applicability of numerical simulation within Abaqus software. Using Genetic Algorithm and Sequential Quadratic Programming (SQP), an optimum shock absorber for the seat of an armored vehicle under conditions of mine explosion has been designed. The analysis of this shock absorber has been performed through numerical simulation in Abaqus software. According to the obtained numerical results, the magnitude of reaction force applied to the occupant's hip, acceleration changes, and HIC parameter for the occupant

have all met the requirements of the relevant standards. Hence, in case of a mine explosion occurring under an armored vehicle, this shock absorber can be efficiently applied beneath the seat. Moreover, the introduced optimization method and numerical simulation can be further extended for miscellaneous applications of shock absorbers such as down the elevator pits for the cases of emergency.

## REFERENCES

- [1] *Test Methodology for Protection of Vehicle Occupants against Anti-Vehicular Landmine Effects*, Technical Report, NATO, 2007.
- [2] *Final Report of HFM-090 Task Group 25 on Test Methodology for Protection of Vehicle Occupants against Anti-Vehicular Landmine Effects*, NATO, 2007.
- [3] Chen Q., Pugno N.M., 2013, In-plane elastic properties of hierarchical nano-honeycombs: The role of the surface effect, *European Journal of Mechanics A/Solids* **37**: 248-255.
- [4] Nakamoto H., Adachi T., Araki W., 2009, In-plane impact behavior of honeycomb structures randomly filled with rigid inclusions, *International Journal of Impact Engineering* **36**: 73-80.
- [5] Tanaka K., Nishida M., Ueki G., 2009, Shock absorption of aluminum honeycombs for in-plane impacts, *28<sup>th</sup> International Congress on High-Speed Imaging and Photonics*.
- [6] Atli-Veltin B., 2009, *Effect of Geometric Parameters on the In-Plane Crushing Behavior of Honeycombs and Honeycombs with Facesheets*, PhD thesis, The Pennsylvania State University.
- [7] Stromsoe J.D., 2011, *Modeling of In-Plane Crushed Honeycomb Cores with Applications to Ramp Down Sandwich Structure Closures*, Ms thesis, San Diego State University.
- [8] Asadi M., Walker B., Shirvani H., 2009, An investigation to compare the application of shell and solid element honeycomb model in ODB, *7<sup>th</sup> European LS-Dyna Conference*.
- [9] Menna C., Zinno A., Asprone D., Prota A., 2013, Numerical assessment of the impact behavior of honeycomb sandwich structures, *Composite Structures* **106**: 326-339.
- [10] Radzai Said M., Tan C.F., 2008, Aluminum honeycomb under quasi-static compressive loading: an experimental investigation, *Suranaree Journal of Science and Technology* **16**: 1-8.
- [11] Chao L.B., Ping Z.G., Jian L.T., 2012, Low strain rate compressive behavior of high porosity closed-cell aluminum foams, *Science China Technological Sciences* **55**: 451-463.
- [12] Shariyat M., Moradi M., Samaee S., 2012, Nonlinear finite element eccentric low-velocity impact analysis of rectangular laminated composite plates subjected to in-phase/anti-phase biaxial preloads, *Journal of Solid Mechanics* **4**(2): 177-194.
- [13] Rezaei Pour Almasi A., Fariba F., Rasoli S., 2015, Modifying stress-strain curves using optimization and finite elements simulation methods, *Journal of Solid Mechanics* **7**(1): 71-82.
- [14] Galehdari S. A., Kadkhodayan M., Hadidi-Moud S., 2015, Analytical, experimental and numerical study of a graded honeycomb structure under in-plane impact load with low velocity, *International Journal of Crashworthiness* **20**(4): 387-400.
- [15] Muhammad A., 2007, *Study of a Compact Energy Absorber*, PhD Thesis, Iowa State University.
- [16] Galehdari S. A., Kadkhodayan M., Hadidi-Moud S., 2015, Analytical numerical and experimental study of energy absorption of graded honeycomb structure under in-plane low velocity impact, *Modares Mechanical Engineering* **14**(15): 261-271.
- [17] Galehdari S. A., Kadkhodayan M., 2015, Study of graded honeycomb structure under in-plane and out of plane impact loading, *17<sup>th</sup> International Mechanical Engineering Conference (ISME 2015)*, Amirkabir University of technology, Tehran, Iran.
- [18] Galehdari S. A., Kadkhodayan M., Hadidi-Moud S., 2015, Low velocity impact and quasi-static in-plane loading on a graded honeycomb structure; experimental, analytical and numerical study, *Aerospace Science and Technology* **47**: 425-433.
- [19] Tabiei A., Nilakantan G., 2014, Reduction of acceleration induced injuries from mine blasts under infantry vehicles, *6th European Ls-Dyna Users' Conference*, Gothenburg, Sweden.
- [20] Sławiński G., Dziewulski P., Niezgoda T., 2015, Investigation of human body exposed to blast wave derived from improvised explosive devices, *Journal of Kones Powertrain and Transport* **22**(4): 287-294.
- [21] Khodarahmi H., 2014, *Investigation, Analysis Tactical Armored Vehicle*, Advanced Ground Defense Technology Research Center, Imam Hossein University .
- [22] Huang H.H., 2009, *Controller Design for Stability and Rollover Prevention of Multi-Body Ground Vehicles with Uncertain Dynamics and Faults*, PhD Thesis, The Ohio State University.
- [23] Michelin Cargobib and Xp 27, 2014, *Technical Documentation*, Michelin Manufacturing Company.
- [24] Wong J.Y., 2001, *Theory of Ground Vehicles*, John Wiley and Sons.
- [25] Halderman J.D., 2012, *Automotive Technology*, Pearson.
- [26] 49 CFR 571.208 – Standard No. 208, 2012, *Occupant Crash Protection*, Cornell University Law School.

- [27] Owen P.L., 2004, *Procedures for Using the Amanda Model in Acceleration Response Studies (Tutorial by Example)*, Army Research Laboratory.
- [28] Panowicz R., Sybilski K., Koodziejczyk D., 2011, Numerical analysis of effects of IDE side explosion on crew of light armored wheeled vehicle, *Journal of Kones Powertrain and Transport* **18**(4): 331-339.